

# Deep sub-threshold $\Xi^-$ production in Ar+KCl reactions at 1.76A GeV

G. Agakishiev<sup>8</sup>, A. Balanda<sup>3</sup>, R. Bassini<sup>9</sup>, D. Belver<sup>15</sup>, A.V. Belyaev<sup>6</sup>, A. Blanco<sup>2</sup>, M. Böhmer<sup>11</sup>, J.L. Boyard<sup>13</sup>, P. Braun-Munzinger<sup>4</sup>, P. Cabanelas<sup>15</sup>, E. Castro<sup>15</sup>, S. Chernenko<sup>6</sup>, T. Christ<sup>11</sup>, M. Destefanis<sup>8</sup>, J. Díaz<sup>16</sup>, F. Dohrmann<sup>5</sup>, A. Dybczak<sup>3</sup>, T. Eberl<sup>11</sup>, L. Fabbietti<sup>11,d</sup>, O. V. Fateev<sup>6</sup>, P. Finocchiaro<sup>1</sup>, P. Fonte<sup>2,a</sup>, J. Friese<sup>11</sup>, I. Fröhlich<sup>7</sup>, T. Galatyuk<sup>7</sup>, J. A. Garzón<sup>15</sup>, R. Gernhäuser<sup>11</sup>, A. Gil<sup>16</sup>, C. Gilardi<sup>8</sup>, M. Golubeva<sup>10</sup>, D. González-Díaz<sup>4</sup>, F. Guber<sup>10</sup>, T. Hennino<sup>13</sup>, R. Holzmann<sup>4</sup>, I. Iori<sup>9,c</sup>, A. Ivashkin<sup>10</sup>, M. Jurkovic<sup>11</sup>, B. Kämpfer<sup>5,b</sup>, K. Kanaki<sup>5</sup>, T. Karavicheva<sup>10</sup>, D. Kirschner<sup>8</sup>, I. Koenig<sup>4</sup>, W. Koenig<sup>4</sup>, B. W. Kolb<sup>4</sup>, R. Kotte<sup>5</sup>, F. Krizek<sup>14</sup>, R. Krücken<sup>11</sup>, W. Kühn<sup>8</sup>, A. Kugler<sup>14</sup>, A. Kurepin<sup>10</sup>, S. Lang<sup>4</sup>, J. S. Lange<sup>8</sup>, K. Lapidus<sup>10</sup>, T. Liu<sup>13</sup>, L. Lopes<sup>2</sup>, M. Lorenz<sup>7</sup>, L. Maier<sup>11</sup>, A. Mangiarotti<sup>2</sup>, J. Markert<sup>7</sup>, V. Metag<sup>8</sup>, B. Michalska<sup>3</sup>, J. Michel<sup>7</sup>, D. Mishra<sup>8</sup>, E. Morinière<sup>13</sup>, J. Mousa<sup>12</sup>, C. Müntz<sup>7</sup>, L. Naumann<sup>5</sup>, J. Otwinowski<sup>3</sup>, Y. C. Pachmayer<sup>7</sup>, M. Palka<sup>4</sup>, Y. Parpottas<sup>12</sup>, V. Pechenov<sup>4</sup>, O. Pechenova<sup>8</sup>, J. Pietraszko<sup>4</sup>, W. Przygoda<sup>3</sup>, B. Ramstein<sup>13</sup>, A. Reshetin<sup>10</sup>, M. Roy-Stephan<sup>13</sup>, A. Rustamov<sup>4</sup>, A. Sadovsky<sup>10</sup>, B. Sailer<sup>11</sup>, P. Salabura<sup>3</sup>, A. Schmah<sup>11,d</sup>, Yu. G. Sobolev<sup>14</sup>, S. Spataro<sup>8</sup>, B. Spruck<sup>8</sup>, H. Ströbele<sup>7</sup>, J. Stroth<sup>7,4</sup>, C. Sturm<sup>7</sup>, M. Sudol<sup>13</sup>, A. Tarantola<sup>7</sup>, K. Teilab<sup>7</sup>, P. Tlusty<sup>14</sup>, M. Traxler<sup>4</sup>, R. Trebacz<sup>3</sup>, H. Tsertos<sup>12</sup>, V. Wagner<sup>14</sup>, M. Weber<sup>11</sup>, M. Wisniowski<sup>3</sup>, T. Wojcik<sup>3</sup>, J. Wüstenfeld<sup>5</sup>, S. Yurevich<sup>4</sup>, Y. V. Zanevsky<sup>6</sup>, P. Zhou<sup>5</sup>

(HADES collaboration)

<sup>1</sup> *Istituto Nazionale di Fisica Nucleare - Laboratori Nazionali del Sud, 95125 Catania, Italy*

<sup>2</sup> *LIP-Laboratório de Instrumentação e Física Experimental de Partículas, 3004-516 Coimbra, Portugal*

<sup>3</sup> *Smoluchowski Institute of Physics, Jagiellonian University of Cracow, 30-059 Kraków, Poland*

<sup>4</sup> *GSI Helmholtzzentrum für Schwerionenforschung GmbH, 64291 Darmstadt, Germany*

<sup>5</sup> *Institut für Strahlenphysik, Forschungszentrum Dresden-Rossendorf, 01314 Dresden, Germany*

<sup>6</sup> *Joint Institute of Nuclear Research, 141980 Dubna, Russia*

<sup>7</sup> *Institut für Kernphysik, Johann Wolfgang Goethe-Universität, 60438 Frankfurt, Germany*

<sup>8</sup> *II. Physikalisches Institut, Justus Liebig Universität Giessen, 35392 Giessen, Germany*

<sup>9</sup> *Istituto Nazionale di Fisica Nucleare, Sezione di Milano, 20133 Milano, Italy*

<sup>10</sup> *Institute for Nuclear Research, Russian Academy of Science, 117312 Moscow, Russia*

<sup>11</sup> *Physik Department E12, Technische Universität München, 85748 München, Germany*

<sup>12</sup> *Department of Physics, University of Cyprus, 1678 Nicosia, Cyprus*

<sup>13</sup> *Institut de Physique Nucléaire (UMR 8608), CNRS/IN2P3 - Université Paris Sud, F-91406 Orsay Cedex, France*

<sup>14</sup> *Nuclear Physics Institute, Academy of Sciences of Czech Republic, 25068 Rez, Czech Republic*

<sup>15</sup> *Departamento de Física de Partículas, Univ. de Santiago de Compostela, 15706 Santiago de Compostela, Spain*

<sup>16</sup> *Instituto de Física Corpuscular, Universidad de Valencia-CSIC, 46971 Valencia, Spain*

<sup>a</sup> *also at ISEC Coimbra, Coimbra, Portugal*

<sup>b</sup> *also at Technische Universität Dresden, 01062 Dresden, Germany*

<sup>c</sup> *also at Dipartimento di Fisica, Università di Milano, 20133 Milano, Italy*

<sup>d</sup> *also at Excellence Cluster Universe, Technische Universität München, 85748 Garching, Germany*

(Dated: October 25, 2018)

We report first results on a deep sub-threshold production of the doubly strange hyperon  $\Xi^-$  in a heavy-ion reaction. At a beam energy of 1.76A GeV the reaction Ar+KCl was studied with the High Acceptance Di-Electron Spectrometer (HADES) at SIS18/GSI. A high-statistics and high-purity  $\Lambda$  sample was collected, allowing for the investigation of the decay channel  $\Xi^- \rightarrow \Lambda\pi^-$ . The deduced  $\Xi^-/(\Lambda + \Sigma^0)$  production ratio of  $(5.6 \pm 1.2_{-1.7}^{+1.8}) \cdot 10^{-3}$  is significantly larger than available model predictions.

PACS numbers: 25.75.-q, 25.75.Dw

The doubly strange  $\Xi^-$  baryon (also known as cascade particle) has, in vacuum, a mass of 1321.3 MeV and decays ( $c\tau = 4.91$  cm) almost exclusively into the  $\Lambda\pi^-$  final state [1]. In elementary nucleon-nucleon (NN) collisions near threshold it must be co-produced with two kaons ensuring strangeness conservation. This requires a minimum beam energy of  $E_{thr} = 3.74$  GeV ( $\sqrt{s_{thr}} = 3.25$  GeV). In heavy-ion collisions, the  $\Xi^-$  yield was measured at various beam energies covered by the RHIC [2], SPS [3, 4] and AGS [5] accelerators. Though cooperative processes in heavy-ion reactions allow for particle production below NN threshold, no

sub-threshold  $\Xi^-$  production was observed so far. Predictions of sub-threshold cascade production at energies available with the heavy-ion synchrotron SIS18 at GSI, Darmstadt, were presented within a relativistic transport model [6]. The cross sections of the strangeness exchange reactions  $\bar{K}Y \rightarrow \pi\Xi$  ( $Y = \Lambda, \Sigma$ ), which are essential for  $\Xi$  creation below the nucleon-nucleon threshold, were taken from a coupled-channel approach based on a flavor SU(3)-invariant hadronic Lagrangian [7]. The  $\Xi^-/\Lambda$  ratio was found to amount to a few times  $10^{-4}$ , varying with system size and beam energy, however, being fairly independent on centrality.

At SIS18 energies, also  $\bar{K}$  production, being a prerequisite of the above strangeness exchange reactions, proceeds below the NN threshold ( $E_{thr} = 2.5$  GeV). A similar strangeness exchange reaction like that relevant for  $\Xi$  production is found to be dominant in sub-threshold  $\bar{K}$  production in heavy-ion collisions [8], i.e.  $\pi Y \rightarrow \bar{K} B$  ( $B = N, \Delta$ ). Thus, medium effects on strange meson properties, like effective anti-kaon masses and hence reduced production thresholds, could strongly influence the  $\Xi$  yield. However, the authors of [6] found the  $\Xi$  yield to be more sensitive to the magnitude of the cross sections of strangeness-exchange reactions than to the medium effects due to modified kaon properties. Generally, the yield of multi-strange particles, measured below their production threshold in NN collisions, is expected to be sensitive to the equation of state (EoS) of nuclear matter. In heavy-ion reactions, the necessary energy for the production of these particles is accumulated via multiple collisions involving nucleons, produced particles and short-living resonances. The corresponding number of such collisions increases with the density inside the reaction zone the maximum of which in turn depends on the stiffness of the EoS.

In this Letter we report on the first observation of sub-threshold  $\Xi^-$  production in heavy-ion collisions. The experiment was performed with the **H**igh **A**cceptance **D**i-**E**lectron **S**pectrometer (HADES) at SIS18 [9]. HADES, primarily designed to measure di-electrons [10], offers excellent hadron identification capabilities, too [11, 12, 13].

A  $^{40}\text{Ar}$  beam of about  $10^6$  particles/s with kinetic energy of  $1.756A$  GeV ( $\sqrt{s_{NN}} = 2.61$  GeV) was incident on a four-fold segmented  $^{nat}\text{KCl}$  target with a total thickness of 5 mm corresponding to 3.3% interaction probability. The beam energy is known with a precision of about  $10^{-3}$ . The energy loss of the beam particles in the target is estimated to be less than 0.5 A MeV per target slice. The position resolution of the primary (reaction) vertex amounts to 0.3 mm in both transverse directions while in beam direction it amounts to 1.5 mm as expected from the finite thickness of the target slices. The data readout was started by a first-level trigger (LVL1) decision, requiring a minimum charged-particle multiplicity  $\geq 16$  in the time-of-flight detectors. The integrated cross section selected by this trigger comprises approximately the most central 35% of the total reaction cross section. About 700 million LVL1 events were processed for the present  $\Xi^-$  investigation.

In the present analysis we identified the  $\Lambda$  hyperons through their decay  $\Lambda \rightarrow p\pi^-$ . Note that the reconstructed  $\Lambda$  yield includes the decay  $\Lambda$ 's of the (slightly heavier)  $\Sigma^0$  baryon decaying exclusively into  $\Lambda$  and a photon [1] which cannot be detected with HADES. Hence, the  $\Lambda$  yield has to be understood as that of  $(\Lambda + \Sigma^0)$  throughout the paper. To allow for  $\Lambda$  selection various cuts on single-particle and two-particle quantities were applied. The most important ones act on geometrical distances, i.e. i) minimum values of the  $p, \pi^-$  track distances to the primary vertex ( $p\text{-VecToPrimVer}$ ,  $\pi_1\text{-VecToPrimVer}$ ), ii) an upper threshold of the  $p\text{-}\pi^-$  minimum track distance ( $p\text{-}\pi_1\text{-MinVecDist}$ ), and iii) a minimum value of the  $\Lambda$  vertex distance to the primary vertex

( $\Lambda\text{-VerToPrimVer}$ ).

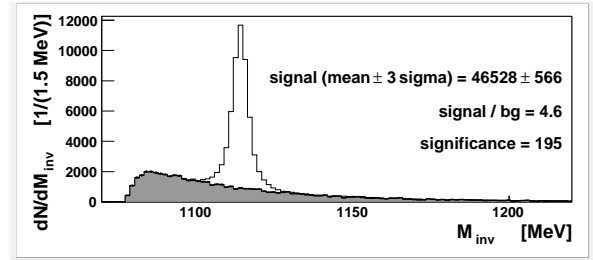


FIG. 1: The  $p\text{-}\pi^-$  invariant mass distribution. Hatched histogram: Scaled combinatorial background produced via event mixing.

With these conditions we first analysed the invariant-mass distribution of proton- $\pi^-$  pairs (Fig. 1). A clear  $\Lambda$  signal could be separated from the combinatorial background (bg) as determined via the event mixing technique. The background normalization was performed over the given invariant-mass range, except a  $\pm 15$  MeV interval around the  $\Lambda$  peak. For a  $\pm 3\sigma$  mass cut around the  $\Lambda$  peak, the signal-to-background ratio and the significance, defined as  $\text{signal}/\sqrt{\text{signal} + \text{bg}}$ , amount to 4.6 and 195, respectively. The total  $\Lambda$  yield for the given cuts is  $N_\Lambda = 46,500 \pm 600$ . Fitting a Gaussian function to the signal, we obtain a mean value of  $(1114.2 \pm 0.1)$  MeV and a width ( $\sigma$ ) of  $(2.7 \pm 0.1)$  MeV.

Taking this high-statistics  $\Lambda$  sample, we started the  $\Xi^-$  investigation by combining - for each event containing a  $\Lambda$  candidate - the  $\Lambda$  with those  $\pi^-$  mesons not already contributing to the  $\Lambda$ . The result was a structureless  $\Lambda\text{-}\pi^-$  invariant mass distribution. Hence, additional conditions were necessary: iv) a lower limit on the 2nd  $\pi^-$  (potential  $\Xi^-$  daughter) track distance to primary vertex ( $\pi_2\text{-VecToPrimVer}$ ), v) an upper limit of the distance of the  $\Xi^-$  pointing vector w.r.t. the primary vertex ( $\Xi\text{-VecToPrimVer}$ ), vi) a maximum value of the minimum track distance of the  $\Lambda$  and the 2nd  $\pi^-$  ( $\pi_2\text{-}\Lambda\text{-MinVecDist}$ ), vii) a minimum value of the distance of the  $\Xi^-$  vertex relative to the primary one ( $\Xi\text{-VerToPrimVer}$ ), and viii) a window of  $\pm 7$  MeV around the  $\Lambda$  mass peak of the  $p\text{-}\pi^-$  invariant mass distribution.

The conditions on the geometrical quantities are summarized in Fig. 2, where the optimum cut values are indicated by arrows. We studied the stability of the signal if more stringent conditions were chosen. Because of the limited statistics all other cuts were kept fixed at the optimum values when varying a single cut quantity. The dependences on the various geometrical distances of experimental data and GEANT [14] simulations (see below) are found in good agreement.

Figure 3 shows the invariant mass distribution of  $\Lambda\text{-}\pi^-$  pairs after applying all conditions. Indeed, a narrow signal shows up on top of a smooth distribution. For an invariant-mass window of  $\pm 10$  MeV (4 bins) around the peak center, we find  $N_{\Xi^-} = 141 \pm 31 \pm 25$  entries to be attributed to  $\Xi^-$  with the given statistical and systematic errors. The signal-to-background ratio and the significance amount to 0.17 and 4.6,

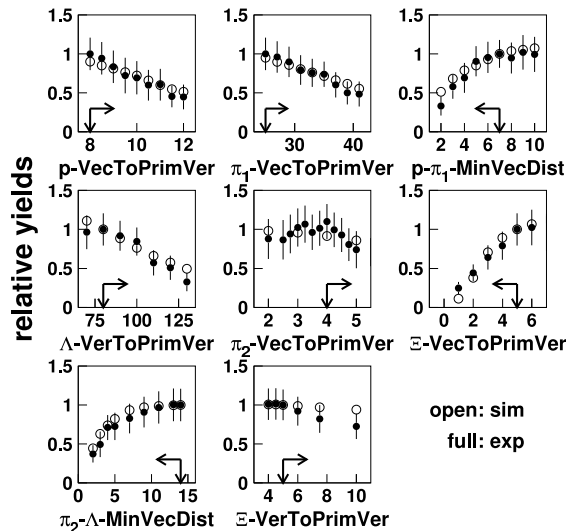


FIG. 2: Relative  $\Xi^-$  yields as a function of the cut value of various  $\Lambda$  and  $\Xi^-$  geometrical distances (see text, units are mm). The full (open) dots display the experimental (simulation) data. The vertical and horizontal arrows indicate the chosen cut values and the region of accepted distances, respectively.

respectively. The given systematic error of the signal is due to the signal variation for various histogram binnings, background normalization regions and mass windows assigned to the signal. These systematic variations are also reflected in the significance of the signal of about 4 – 6. The full line in the bottom panel of Fig. 3 represents a Gaussian fit to the signal. The mean value of  $(1320 \pm 1)$  MeV is well in agreement with the PDG value of 1321.3 MeV [1]. Taking into account the bias due to the rather large bin size of 5 MeV to be used for statistical reasons, the peak width ( $\sigma$ ) of  $(4 \pm 1)$  MeV is in fair agreement with GEANT simulations which predict for  $\Lambda$  and  $\Xi^-$  baryons almost equal values of about 2.5 MeV. In order to ensure that not a fake signal is selected, we performed a  $\Lambda$ -side-band analysis. No signal was found when choosing instead of condition viii) a window in the  $p\text{-}\pi^-$  invariant mass of  $10 < |M_{p\pi^-} - \langle M_\Lambda \rangle| < 25$  MeV. Furthermore, when dividing randomly the data sample into two sub-samples, the  $\Xi^-$  sub-yields were found - within errors - compatible with half of the above quoted total yield.

Corrections for the finite acceptances and reconstruction efficiencies were deduced from simulations. Thermal  $\Lambda$ 's ( $\Xi^-$ 's), characterized by the temperature parameter  $T_\Lambda$  ( $T_{\Xi^-}$ ) were generated with the event generator Pluto [15]. The experimental  $\Lambda$  rapidity distribution is found slightly broader than the thermal model distribution [11, 16]. Consequently, in Pluto we allowed also for anisotropic, i.e. longitudinally elongated, phase-space distributions. For this purpose, an additional width parameter of Gaussian rapidity distributions,  $\sigma_y$ , is taken into account. The  $\Lambda$  parameters are chosen such that the simulation reproduces both, the experimental values of the effective inverse slope parameter at mid-rapidity,  $T_{eff,\Lambda} = 95$  MeV, and the rapidity width,  $\sigma_{y,\Lambda} = 0.42$

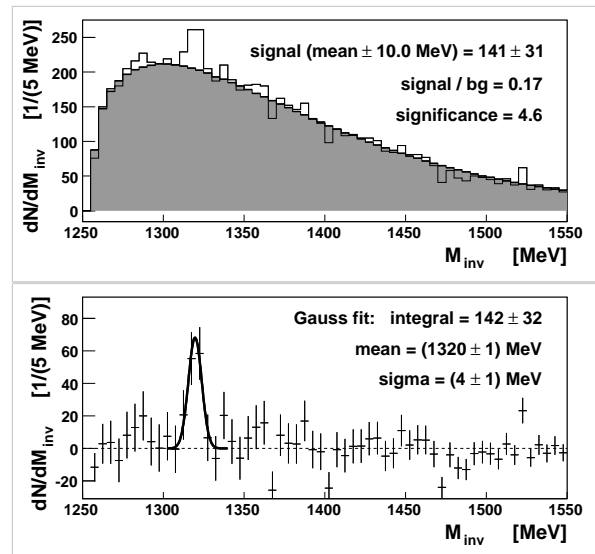


FIG. 3: Top: The same as Fig. 1, but for  $\Lambda\text{-}\pi^-$  pairs. Bottom: The invariant mass distribution after background subtraction. The full line represents a Gaussian fit to the  $\Xi^-$  signal.

[11, 12]. Since the phase-space distribution of the  $\Xi^-$  is not known, we investigated its geometrical acceptance for a broad range of the transverse and longitudinal shape parameters, i.e. the inverse slope and rapidity width,  $T_{eff,\Xi^-} = (95 \pm 25)$  MeV and  $\sigma_{y,\Xi^-} = 0.34 \pm 0.09$ , respectively. Here, the  $\Lambda$  inverse slope serves as a reference value. The lower limit of  $T_{eff,\Xi^-}$  matches the measured inverse slope parameter of  $K^-$  mesons [12, 13] being essential for producing  $\Xi$  hyperons via strangeness-exchange processes (see above), while the upper limit is set by a similar interval above the  $\Lambda$  slope. We assumed the rapidity width of  $\Xi^-$ 's to be larger than the width of thermal  $\Xi^-$ 's with a temperature of 95 MeV but smaller than that of  $\Lambda$ 's. This choice is substantiated by two facts: Firstly, for a thermal rapidity distribution, the width approximately scales with the square root of mass ( $\sigma_y = \sqrt{T/m_0 c^2}$ ), and secondly, the cascade particle may carry less longitudinal momentum than the  $\Lambda$  hyperon, since it contains only one light quark which arises from projectile nucleons. With the given parameters and their ranges, we calculated the HADES acceptance (including the branching ratio for the decay  $\Lambda \rightarrow p\pi^-$ ) for the  $\Lambda$  to  $\epsilon_{acc,\Lambda} = 0.160 \pm 0.009$ , and for the  $\Xi^-$  to  $\epsilon_{acc,\Xi^-} = (9.6^{+2.3}_{-2.1}) \cdot 10^{-2}$ . The simulation data are processed through GEANT modeling the detector response. The GEANT data were embedded into real experimental data and processed through the full analysis chain. Relating the outputs after cuts to the corresponding inputs, the  $\Lambda$  and  $\Xi^-$  reconstruction efficiencies were estimated to  $\epsilon_{eff,\Lambda} = (6.1 \pm 0.3) \cdot 10^{-2}$  and  $\epsilon_{eff,\Xi^-} = (5.5 \pm 0.5) \cdot 10^{-2}$ , respectively. We proved our acceptance and efficiency corrections by extracting the lambda yield [11] which is found to be in agreement with existing data [16]. With the above correction factors, the ratio of  $\Xi^-$  and  $\Lambda$  production yields can be determined. Such a ratio, when derived from the same data

analysis, has the advantage that systematic errors cancel to a large extent. The ratio is calculated as

$$\frac{P_{\Xi^-}}{P_{\Lambda+\Sigma^0}} = \frac{N_{\Xi^-}}{N_{\Lambda}} \frac{\epsilon_{acc,\Lambda}}{\epsilon_{acc,\Xi^-}} \frac{\epsilon_{eff,\Lambda}}{\epsilon_{eff,\Xi^-}} = (5.6 \pm 1.2_{-1.7}^{+1.8}) 10^{-3}, \quad (1)$$

where statistical and systematic errors are given, resulting from adding the individual ones quadratically. The statistical error in (1) is dominated by the 20% error of the  $\Xi^-$  signal while the systematic error is governed by the stability of the signal against cut and background variation and by the range of the parameters  $T_{\Xi^-}$  and  $\sigma_{y,\Xi^-}$  entering the simulation.

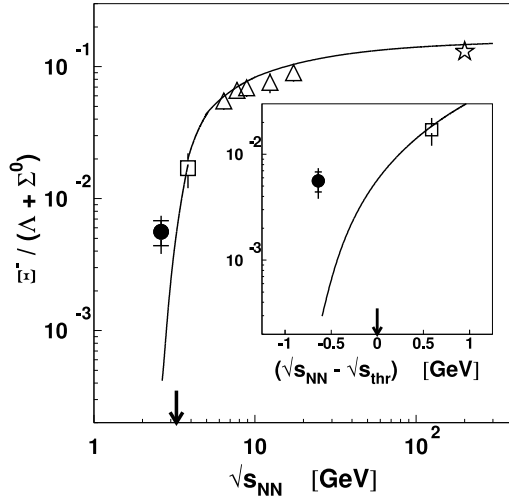


FIG. 4: The yield ratio  $\Xi^- / (\Lambda + \Sigma^0)$  as a function of  $\sqrt{s_{NN}}$  or  $\sqrt{s_{NN}} - \sqrt{s_{thr}}$  (inset). The arrow gives the threshold in free NN collisions. The open star, triangles and square represent data for central Au+Au and Pb+Pb collisions measured at RHIC [2], SPS [3, 4] and AGS [5], respectively. The filled circle shows the present ratio (1) for Ar+KCl reactions at 1.76A GeV (statistical error within ticks, systematic error as bar). Full line: Statistical model for Au+Au [17].

The deduced  $\Xi^- / \Lambda$  ratio (1) may be compared with the corresponding ratios at higher energies [2, 3, 4, 5]. Figure 4 shows a compilation of  $\Xi^- / \Lambda$  ratios as a function of  $\sqrt{s_{NN}}$ . The displayed data represent the most central 5-10% of collisions of Au+Au or Pb+Pb. At RHIC and SPS energies hardly any centrality dependence of the  $\Xi^- / \Lambda$  ratio was observed [2, 3]. So far, the lowest energy at which a  $\Xi^- / \Lambda$  ratio is available is  $\sqrt{s_{NN}} = 3.84$  GeV, i.e. an excess energy of +600 MeV above the NN threshold [5]. The corresponding ratio, measured at the AGS at a beam energy of 6A GeV, is found to increase slightly with centrality. For central (semi-central) collisions it is about three (two) times larger than our value. Indeed, a steep decline of the  $\Xi^- / \Lambda$  production ratio is expected below threshold, where now the first data point is available. This allows for comparisons to model calculations.

The  $\Xi^- / \Lambda$  ratio has been estimated within a statistical approach [17]. While RHIC [2], SPS [3, 4] and AGS [5] data are well described, the present experimental  $\Xi^- / \Lambda$  ratio is underestimated (cf. Fig. 4). A similar small ratio is derived [18]

when taking - instead of the calculations along the schematic freeze-out curve for Au+Au [17] - the optimum input parameters (i.e. temperature, charge and baryon chemical potentials, strangeness correlation volume) following from the best fit to all HADES particle yields in Ar+KCl at 1.76A GeV [11, 13]. Finally, recent predictions within a transport approach [6] (soft EoS with incompressibility  $K_0 = 194$  MeV at normal nuclear matter density) yield a  $\Xi^- / \Lambda$  ratio of a few times  $10^{-4}$ , comparable to the statistical model.

In summary, we observed the production of the doubly strange cascade hyperon  $\Xi^-$  in collisions of Ar+KCl at 1.76A GeV with a significance of about five. For the first time, using the HADES detector at SIS18/GSI, this hyperon was measured below the threshold in free nucleon-nucleon collisions, i.e. at  $\sqrt{s_{NN}} - \sqrt{s_{thr}} = -640$  MeV. Comparing the experimental  $\Xi^- / (\Lambda + \Sigma^0)$  ratio to the predictions of a statistical model and a transport approach, both ones underestimate the experimental ratio. We conclude that I) the conditions for the applicability of present statistical models might be not fulfilled for such rare-particle production in small systems far below threshold, and that II) in transport approaches a better understanding is necessary of the strangeness-exchange reactions conjectured as the dominant process for cascade production below and close to threshold. Other explanations for the unexpectedly high  $\Xi^-$  yield, like modifications of strange hadrons in the nuclear medium, should be investigated.

The HADES collaboration gratefully acknowledges the support by BMBF grants 06TM970I, 06GI146I, 06F-140, and 06DR135 (Germany), by GSI (TM-FR1, GI/ME3, OF/STR), by grants GA AS CR IAA100480803 and MSMT LC 07050 (Czech Republic), by grant KBN 5P03B 140 20 (Poland), by INFN (Italy), by CNRS/IN2P3 (France), by grants MICYT FPA2000-2041-C02-02 and XUGA PGID T02PXIC20605PN (Spain), by grant UCY-10.3.11.12 (Cyprus), by INTAS grant 06-1000012-8861 and EU contract RII3-CT-2004-506078.

- [1] C. Amsler *et al.* (PDG), Phys. Lett. B **667**, 1 (2008).
- [2] J. Adams *et al.* (STAR), Phys. Rev. Lett. **98**, 062301 (2007).
- [3] F. Antinori *et al.* (NA57), Phys. Lett. B **595**, 68 (2004).
- [4] C. Alt *et al.* (NA49), Phys. Rev. C **78**, 034918 (2008).
- [5] P. Chung *et al.* (E895), Phys. Rev. Lett. **91**, 202301 (2003).
- [6] L.-W. Chen, C. M. Ko, Y. Tzeng, Phys. Lett. B **584**, 269 (2004).
- [7] C. H. Li, C. M. Ko, Nucl. Phys. **A712**, 110 (2002).
- [8] Ch. Hartnack, H. Oeschler, J. Aichelin, Phys. Rev. Lett. **90**, 102302 (2003).
- [9] G. Agakishiev *et al.* (HADES), arXiv:0902.3478.
- [10] G. Agakishiev *et al.* (HADES), Phys. Rev. Lett. **98**, 052302 (2007).
- [11] A. Schmah, PhD thesis, Techn. Universität Darmstadt (2008).
- [12] L. Fabbietti, J. Phys. G: Nucl. Part. Phys. **36**, 064005 (2009).
- [13] G. Agakishiev *et al.* (HADES), arXiv:0902.3487.
- [14] GEANT 3.21, <http://consult.cern.ch/writeup/geant/> (1993).
- [15] I. Fröhlich *et al.*, Proc. of Science, PoS(ACAT)076 (2007).
- [16] M. Merschmeyer *et al.* (FOPI), Phys. Rev. C **76**, 024906 (2007).
- [17] A. Andronic, P. Braun-Munzinger, K. Redlich, Nucl. Phys. **A765**, 211 (2006).
- [18] A. Andronic, private communication.